Eur. Phys. J. A **7**, 391–396 (2000)

THE EUROPEAN PHYSICAL JOURNAL A

Prompt contributions to the dilepton yield in heavy ion collisions

J. Hüfner[1,2], Yu.P. Ivanov[1,2,3], B.Z. Kopeliovich[2,3], J. Raufeisen[1,2]

[1] Institut für Theoretische Physik der Universität, Philosophenweg 19, 69120 Heidelberg, Germany
[2] Max-Planck Institut für Kernphysik, Postfach 103980, 69029 Heidelberg, Germany
[3] Joint Institute for Nuclear Research, Dubna, 141980 Moscow Region, Russia

Received: 1 December 1999 / Revised version: 18 February 2000
Communicated by A. Schäfer

Abstract. The mass spectrum is calculated for those dileptons which are produced in the early phase of a heavy ion collisions via the direct production $NN \to l^+l^-X$ and via the Compton process $GN \to l^+l^-X$ with prompt gluons radiated in preceding NN interactions. Both mechanisms produce a mass spectrum which decreases steeply with invariant mass of the l^+l^- pair and which is below the CERES data for Pb-Au collisions by about one order of magnitude.

PACS. 13.85.Qk Inclusive production with identified leptons, photons, or other nonhadronic particles – 24.85.+p Quarks, gluons, and QCD in nuclei and nuclear processes – 12.38.Bx Perturbative calculations – 12.38.Lg Other nonperturbative calculations

1 Introduction

Dileptons with invariant mass below 1 GeV have been measured in proton-nucleus [1] and heavy ion collisions [2,3] at the CERN SpS accelerator. For heavy ions (laboratory energy 158 A GeV) a sizable enhancement of the order of a factor three has been observed over what is calculated from the e^+e^- decay of the hadrons in the final state. Also the observed shape is very different from the calculated one. The data have not yet found an unambiguous explanation. Most theories locate the origin for the observed dileptons in the hot and dense phase of hadrons [4]- [12]. This phase is rather late in the time evolution of a heavy ion collision.

In this note, we take the opposite point of view and investigate the mass spectrum of the dileptons which arise from the very early stages of the heavy ion reaction in which partons are the relevant degrees of freedom. We calculate (i) the direct production $NN \to l^+l^-X$ in the light cone approach and in a parton model and (ii) the lepton production via a gluonic Compton process $GN \to l^+l^-X$ from prompt gluons which are radiated in preceding nucleon-nucleon interactions. These prompt gluons have been recently identified as as an important source for charmonium suppression in heavy ion collisions [13]. This observation has triggered the present investigation.

2 Direct production of dileptons: light cone approach versus parton model

First we discuss the direct production of lepton pairs, which is already calculated using a parton model and perturbative QCD [14]. However, in the experiments under consideration, the invariant masses of the observed pairs are below 1 GeV. In this domain pQCD may be questionable and we use a phenomenology based on the light cone approach which includes nonperturbative effects [15–17].

In the light cone approach, the Drell-Yan type process illustrated by one of the possible Feynman diagrams in Fig. 1a is viewed in the target rest frame, where it looks like bremsstrahlung from a NN collision. The incident quark from N_1 scatters off a nucleon N_2 in the target and radiates a massive photon γ^* which then decays into a lepton pair. The cross section takes the form [15,19,16]

$$\frac{d\sigma(qN \to \gamma^* qN)}{d(\ln \alpha)} = \int d^2 r_T |\Psi_{\gamma^* q}(\alpha, \boldsymbol{r}_T)|^2 \sigma_{q\bar{q}}(\alpha r_T, s), \quad (1)$$

where α is the fraction of the light cone momentum of the quark carried away by the photon and r_T is the transverse separation between the quark and the photon. $\Psi_{\gamma^* q}(\alpha, \boldsymbol{r}_T)$ is the light cone wave function for the transition $q \to q\gamma^*$. We give the explicit expressions for transverse (T) and longitudinal (L) photons

$$|\Psi_{\gamma^* q}(\alpha, \boldsymbol{r}_T)|^2 = |\Psi^T_{\gamma^* q}(\alpha, \boldsymbol{r}_T)|^2 + |\Psi^L_{\gamma^* q}(\alpha, \boldsymbol{r}_T)|^2, \quad (2)$$

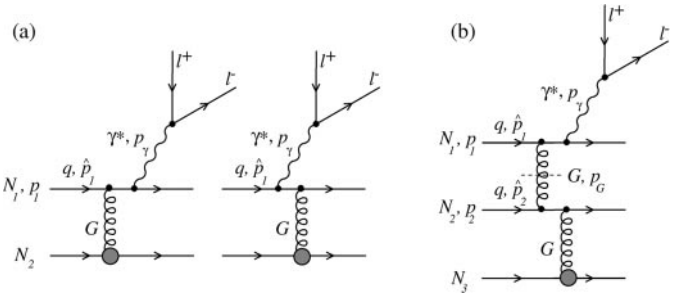

Fig. 1. Diagrams for the two mechanisms for l^+l^- production considered in this paper. (a) Dilepton production in NN collisions which can be viewed as bremsstrahlung in qq scattering (light cone approach) or as gluonic Compton scattering ($Gq \to \gamma^* q$) from the gluon cloud of the second nucleon (parton approach). (b) Dileptons from prompt gluons $Gq \to \gamma^* q$, where the on-mass-shell gluon G (crossed by a dashed line) is produced in another NN collision

$$|\Psi^T_{\gamma^* q}(\alpha, \boldsymbol{r}_T)|^2 = \frac{\alpha_{em}}{\pi^2}\Big\{ m_q^2 \alpha^4 K_0^2(\varepsilon r_T) + \left[1 + (1-\alpha)^2\right] \varepsilon^2 K_1^2(\varepsilon r_T) \Big\}, \quad (3)$$

$$|\Psi^L_{\gamma^* q}(\alpha, \boldsymbol{r}_T)|^2 = \frac{2\alpha_{em}}{\pi^2} M^2 (1-\alpha)^2 K_0^2(\varepsilon r_T) \quad (4)$$

with $\varepsilon^2 = m_q^2\alpha^2 + M^2(1-\alpha)^2$, where m_q is the quark mass and $M^2 = p_\gamma^2$. Note that although there is only a single quark in the initial state the cross section (1) for radiation of a photon depends on the cross section $\sigma_{q\bar{q}}(\alpha r_T, s)$ for the scattering of a $q\bar{q}$ dipole off a proton. Here, αr_T is the transverse separation of the dipole and s is the *c.m.* energy of the quark nucleon system squared. This can be understood as follows [15,16]. The physical quark is represented as a coherent superposition of different Fock states. In our case, we take only the bare quark q and the $q\gamma^*$ states into account. If these two Fock states would scatter with the same amplitude off the target, coherence would be undisturbed and no radiation produced. The radiation amplitude is proportional to the difference between the scattering amplitudes of the two Fock components. The dipole cross section enters, because of the interference between the two graphs in Fig. (1a). The impact parameter of the projectile quark serves as center of gravity for the $q\gamma^*$ fluctuation. The difference in impact parameter between the parent quark and the quark in the fluctuation is αr_T. Therefore, the two graphs have a relative phase factor $\exp(i\alpha \boldsymbol{r}_T \cdot \boldsymbol{p}_T)$. The antiquark appears, when one takes the complex conjugate of one of the graphs. It is now easy to see, that in the absolute square of the two graphs, the color screening factor $[1-\exp(i\alpha \boldsymbol{r}_T \cdot \boldsymbol{p}_T)]$ of $\sigma_{q\bar{q}}(\alpha r_T, s)$ emerges from the four different possible attachements of the two gluons. Therefore the dipole cross section appears in (1), although there is no physical dipole in the system.

Perturbative QCD predicts $\sigma_{q\bar{q}}(r_T, s) \propto r_T^2$ for $r_T \to 0$. Indeed, a colorless $q\bar{q}$ dipole can interact only via its color dipole moment. However, since we are interested in the low mass region, which corresponds to rather large separations r_T, we rely on phenomenology and employ the modification [17] of the saturation model of [20]

$$\sigma_{q\bar{q}}(r_T, s) = \sigma_0(s)\left[1 - \exp\left(-\frac{r_T^2}{r_0^2(s)}\right)\right], \quad (5)$$

where $r_0(s) = 0.88(s/s_0)^{-0.14}$ fm, $s_0 = 1000$ GeV^2. This cross section is proportional to r_T^2 for $r_T \to 0$, but flattens off at large r_T. The energy dependence correlates with r_T. At small r_T the dipole cross section rises faster with energy than at large separations:

$$\sigma_0(s) = \sigma_{tot}^{\pi p}(s)\left(1 + \frac{3r_0^2(s)}{8\langle r_{ch}^2\rangle_\pi}\right), \quad (6)$$

where $\sigma_{tot}^{\pi p}(s) = 23.6(s/s_0)^{0.08}$ mb and $\langle r_{ch}^2\rangle_\pi = 0.44$ fm^2. With this choice, value and energy dependence of the total cross section for pion proton scattering is automatically reproduced. This cross section also allows to describe well the structure function F_2 in DIS in a wide interval of energies and Q^2 [17].

The partonic cross section (1) has to be embedded into the hadronic process. The cross section of direct dilepton production takes the form

$$\frac{d^2\sigma^D}{dMdy} = \frac{2\alpha_{em}}{3\pi M}\sum_q e_q^2 \int_{x_1}^1 d\alpha \frac{x_1}{\alpha^2}\left[f_q\left(\frac{x_1}{\alpha}\right) + f_{\bar{q}}\left(\frac{x_1}{\alpha}\right)\right] \cdot \frac{d\sigma(qN \to \gamma^* qN)}{d(\ln\alpha)} + \Big\{y \Rightarrow -y\Big\}, \quad (7)$$

where y is the rapidity of the lepton pair in the c.m. frame and $x_1 = (\sqrt{x_F^2 + 4M^2/s} + x_F)/2$. The first term corresponds to radiation from the projectile quarks and the second term to radiation from the target quarks (see Fig 1a), which corresponds to replacement $y \to -y$ in the first term. Since the dominant contribution to the cross section comes from large values of x_1/α, we neglect antiquarks in the projectile, $f_{\bar{q}}(x_1/\alpha) \equiv 0$. We parameterize the valence quark distribution in the well known form

$$f_u(x) = \frac{C_u}{\sqrt{x}}(1-x)^3, \quad (8)$$

$$f_d(x) = \frac{C_d}{\sqrt{x}}(1-x)^4, \quad (9)$$

where $C_{u,d}$ are defined by the normalization to the number of valence quarks $N_{u,d}$ in a nucleon

$$\int_0^1 dx\, f_{u,d}(x) = N_{u,d}. \quad (10)$$

In the case of the proton-nucleus (pA) and nucleus-nucleus (AB) collisions the cross section of the direct production is given by the integration of the nuclear densities $\rho_{A,B}$ over the impact parameter

$$\frac{d^2\sigma^D_{AB}}{dMdy} = \int d\mathbf{b}\int d\mathbf{s}\int_{-\infty}^{\infty} dz_A\, \rho_A(\mathbf{s}, z_A) \cdot \int_{-\infty}^{\infty} dz_B\, \rho_B(\mathbf{b}-\mathbf{s}, z_B)\frac{d^2\sigma_{NN}}{dMdy} = AB\frac{d^2\sigma_{NN}}{dMdy}. \quad (11)$$

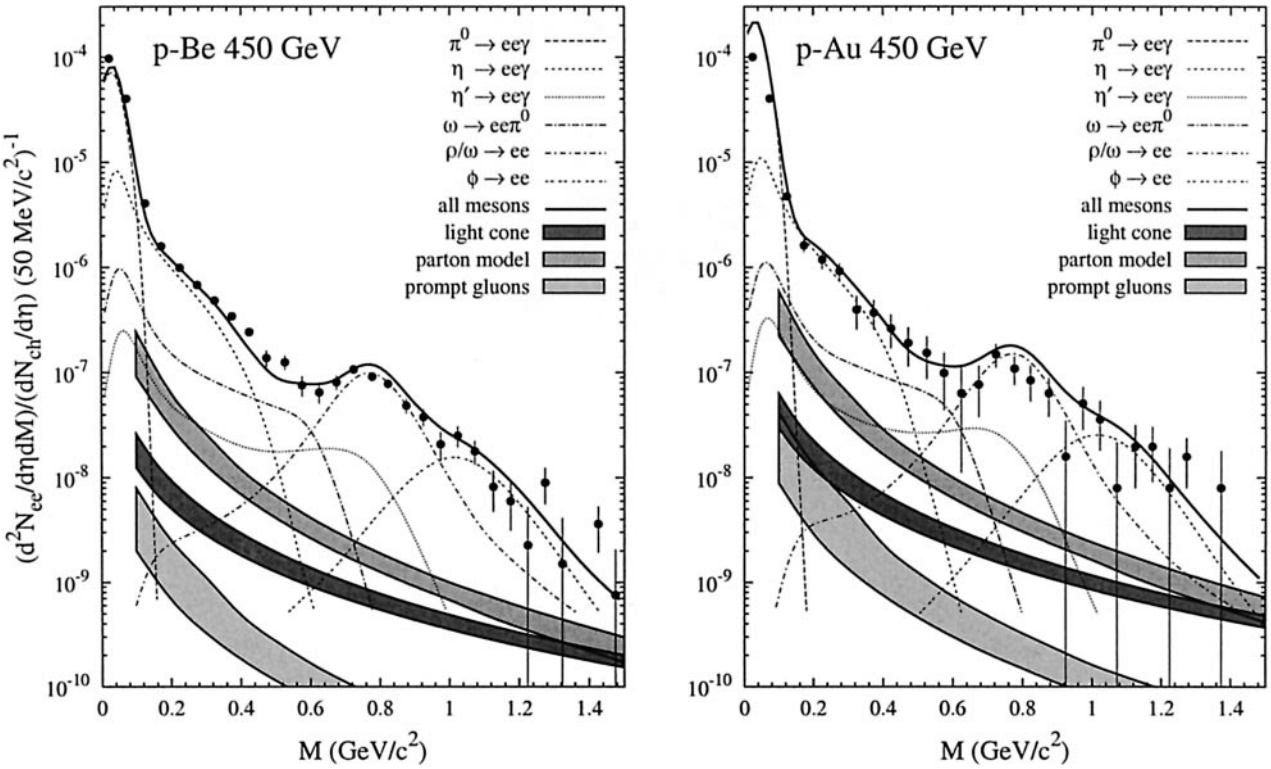

Fig. 2. Data [1] on dilepton events in p-Be and p-Au scattering together with predictions from different mechanisms. The various curves correspond to meson decay channels. The shaded areas represent our results for direct production (in the light cone and the parton model approaches) and via prompt gluons (see Sect. 3): the upper limits correspond to the quark mass $m_q = 150$ MeV and the lower ones to $m_q = 300$ MeV

In this expression we neglect small shadowing effects. To obtain the rate of the dilepton events per interaction one has to divide expression (11) by the total cross section, which can be calculated using the Glauber expressions

$$\sigma_{pA} = \int d\mathbf{b} \left[1 - \exp\left(-\sigma_{NN}^{in} T_A(\mathbf{b})\right)\right], \tag{12}$$

$$\sigma_{AB} = \int d\mathbf{b} \left[1 - \exp\left(-\sigma_{NN}^{in} \int d\mathbf{s}\, T_A(\mathbf{s})\, T_B(\mathbf{b}-\mathbf{s})\right)\right], \tag{13}$$

where $\sigma_{NN}^{in} \approx 30$ mb denotes the inelastic NN cross section and we used the standard Woods-Saxon parameterization [18] for the nuclear density $\rho_{A,B}$ in

$$T_{A,B}(\mathbf{b}) = \int_{-\infty}^{\infty} dz\, \rho_{A,B}(\mathbf{b}, z). \tag{14}$$

There are still two sources of uncertainty:

- The dipole cross section $\sigma_{q\bar{q}}(r_T, s)$ cannot be calculated perturbatively at large transverse separations, which are important in the small mass region, however. We employ the phenomenological expression (5).
- The light cone wave function $\Psi_{\gamma q}(\alpha, \boldsymbol{r}_T)$ depends on the mass m_q of the quark. To illustrate its influence we calculate the cross sections for the two extreme cases of the constituent quark mass $m_q = 150$ MeV and $m_q = 300$ MeV.

Our results for proton (p-Be, p-Au) and heavy ion (Pb-Au) scattering are shown in Figs. 2,3 under the label "light cone". The border lines of the shadowed areas correspond to different assumptions about the constituent mass m_q (150 MeV and 300 MeV for the upper and lower lines, respectively). We believe, that also a different dipole cross section cannot produce values, which are significantly out of the shaded area, because $\sigma_{q\bar{q}}$ is well constrained to describe the structure function F_2 and hadronic cross sections.

It is instructive to compare these results with predictions from a parton model which treats direct radiation of the lepton pair as Compton scattering of a target gluon on a beam quark (or *vice versa*). This way of description should be identical to one employed above (as one can see from Fig. 1). However, all phenomenological modifications introduced via the effective $q\bar{q}$ cross sections are missing. The subprocess $qG \to l^+l^-X$ is then calculated perturbatively with the help of the valence quark and gluon distributions in the proton.

The main uncertainties in this case originate from:

- Possible failure of pQCD calculations for the soft Compton amplitude.
- Poor knowledge of the gluon distribution function, especially at a soft scale.

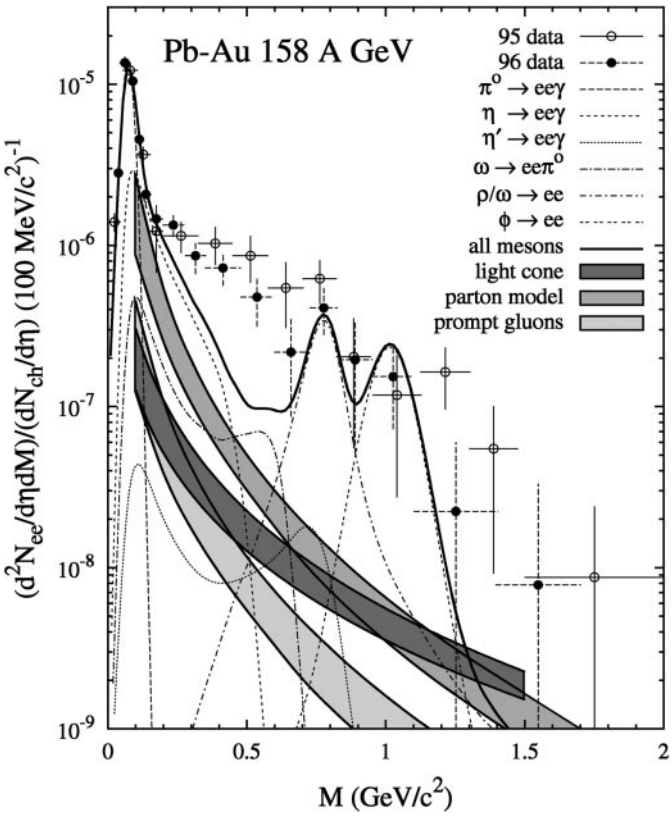

Fig. 3. Data [2,3] on dilepton events in Pb-Au scattering. The different curves correspond to meson decay channels. The shaded areas are our results for direct production in the light cone approach and via prompt gluons (see Sect. 3): the upper limits correspond to the quark mass $m_q = 150$ MeV and the lower ones to $m_q = 300$ MeV. Both processes contribute separately to the dilepton production and therefore their contributions have to be added

We use the following gluon distribution function,

$$f_G(x) = \frac{C_G}{x^{1.1}}(1-x)^5, \tag{15}$$

where C_G is defined from the condition that gluons carry a half of the nucleon momentum

$$\int_0^1 dx\, x\, f_G(x) = \frac{1}{2}. \tag{16}$$

The pQCD calculation of the Compton amplitude is similar to that for an interaction with on mass shell gluons presented in the next section.

The results for proton (p-Be, p-Au) and heavy ion (Pb-Au) scattering are shown in Figs. 2, 3. At low M the results of pQCD (labeled as "parton model") are higher than those from the light cone calculations but start to agree for $M \gtrsim 1$ GeV. The reason for this is that the saturation of the dipole cross section becomes important at small M, and the cross section decays weaker than $1/M^3$. Although the parton model results are supposed to coincide with the predictions of the light-cone approach different approximations are used and the amount of disagreement between the results may serve as a measure of theoretical uncertainty. Nevertheless, we believe that light cone prediction is more reliable.

The data in Figs. 2 and 3 have been measured in a pseudorapidity interval of $2.1 < \eta < 2.65$, while our calculations have been performed for rapidity $y = 2.4$. Note that the data are also subject to p_T cuts, which exclude very small transverse momenta, $p_T < 50$ MeV. These cuts are not included in our calculation. In the region of our interest ($M = 0.2$–0.8 GeV) however both approaches underestimate the experimental data by at least a factor of 10. We therefore believe, that also a more careful calculation would not change our results.

3 Secondary interactions of radiated "prompt" gluons

The second process, labeled "prompt gluons", considers gluons which are radiated in an elementary NN collision and which convert into a virtual photon via gluonic Compton scattering on another nucleon. To estimate their contribution to the dilepton pair production we start with the elementary Compton subprocess $G\,q \to \gamma^*\,q$ (see the upper part of Fig. 1b where the on-mass-shell gluon is marked by a dashed line). The invariant mass distribution for l^+l^- from this process can be expressed in terms of standard kinematic variables $\hat{s} = (\hat{p}_1 + p_G)^2$, $\hat{t} = (\hat{p}_1 - p_\gamma)^2$ and $\hat{u} = (p_G - p_\gamma)^2$ as follows (we use expressions from [14] with substitutions $\hat{s} \Rightarrow \hat{s} - m_q^2$, $\hat{t} \Rightarrow \hat{t} - m_q^2$, $\hat{u} \Rightarrow \hat{u} - m_q^2$)

$$\frac{d^2\sigma(qG \to l^+l^-X)}{dM^2 d\hat{t}} = \frac{\alpha_{em}^2 \alpha_s e_q^2}{9M^2(\hat{s}-m_q^2)^2} \cdot \left[\frac{(\hat{s}-m_q^2)^2 + (\hat{t}-m_q^2)^2 + 2M^2(\hat{u}-m_q^2)}{-(\hat{s}-m_q^2)(\hat{t}-m_q^2)}\right]. \tag{17}$$

If one neglects the transverse momenta of the initial particles, the cross section for the lepton pair production by the gluonic Compton process on a quark takes the following form when going from the variable $\hat{t}$ to rapidity y (for notations see Fig.1b)

$$\frac{d^2\sigma(qG \to l^+l^-X)}{dM dy} = 2M \left|\frac{d\hat{t}(y)}{dy}\right| \frac{d^2\sigma(qG \to l^+l^-X)}{dM^2 d\hat{t}}, \tag{18}$$

where

$$\hat{t}(y) = m_q^2 + M^2 - (\hat{s} + M^2 - m_q^2) \cdot \left[\frac{\hat{E}_1 - \hat{p}_1^{\parallel}\tanh(y)}{\hat{E}_1 + E_G - (\hat{p}_1^{\parallel} + p_G^{\parallel})\tanh(y)}\right]. \tag{19}$$

To obtain the cross section for a nucleon one has to integrate expression (19) over the quark distributions f_q and mean number of gluons n_G, which are radiated by quarks from a projectile nucleon in an interaction with a target nucleon. To calculate the prompt gluon spectrum

we use the perturbative evaluation for the cross section of gluon radiation [16]

$$\frac{d^2\sigma(q\to qG)}{d\alpha dk^2} = \frac{3\alpha_s C}{\pi}\frac{2m_q^2\alpha^4k^2+[1+(1-\alpha)^2](k^4+\alpha^4m_q^4)}{(k^2+\alpha^2m_q^2)^4} \cdot\left[\alpha+\frac{9}{4}\frac{1-\alpha}{\alpha}\right], \quad (20)$$

where $k^2 \equiv \mathbf{p}^2_{\perp G}$, C is the factor of the dipole approximation for the cross section of a $q\hat{q}$ pair with a nucleon (in this energy range $C \approx 3$ [21]) and α is the fraction of the quark light cone momentum carried by the gluon

$$\alpha \equiv \frac{p_G^+}{\hat{p}_2^+} = \frac{\sqrt{p_G^{\parallel 2}+k^2}+p_G^{\parallel}}{\hat{p}_2^+}. \quad (21)$$

Here light cone variables $p_i^+ \equiv E_i + p_i^{\parallel}$ are used. By integrating (20) over k^2 one obtains the gluon distribution over longitudinal momentum

$$\frac{dn_G}{dp_G^{\parallel}} = \frac{3}{\sigma_{NN}^{in}}\int_{k^2_{min}}^{k^2_{max}} dk^2 \left|\frac{d\alpha}{dp_G^{\parallel}}\right| \frac{d^2\sigma(q\to qG)}{d\alpha dk^2}, \quad (22)$$

where

$$k^2_{max} = (\hat{p}_2^+)^2 - 2\hat{p}_2^+ p_G^{\parallel} \quad (23)$$

$$k^2_{min} = \max\left[\Lambda^2, \eta\xi - \eta^2\left(\xi + m_q^2\right)\right], \quad \eta = \frac{2\hat{p}_2^+ p_G^{\parallel}+\xi}{(\hat{p}_2^+)^2+\xi+m_q^2}, \quad \xi = \hat{p}_2^+/\Delta z \quad (24)$$

and $\Lambda \approx 250$ MeV is the pQCD parameter. Expression (24) is obtained from the restriction that the gluon formation length l_G should be shorter than the mean free path of a quark $\Delta z \approx 0.6$ fm

$$l_G = \frac{\alpha(1-\alpha)\hat{p}_2^+}{\alpha^2m_q^2+k^2} \le \Delta z. \quad (25)$$

For each fixed quark momentum $\hat{p}_2^{\parallel}$ (22) gives the gluon distribution as a function of $p_G^{\parallel}$ in the interval from zero up to

$$p_{G\,max}(\hat{p}_2^{\parallel}) = \frac{(\hat{p}_2^+)^2-\Lambda^2}{p_q^+}. \quad (26)$$

To obtain the prompt gluon distribution radiated by a nucleon with momentum p_2 as a function of $x_G = p_G^{\parallel}/p_2$ one has to integrate expression (22) with the quark distribution functions

$$\frac{dn_G}{dx_G} = \sum_q \int_0^1 dx_2 f_q(x_2) \cdot\int_0^{p_{G\,max}(x_2p_2)} dp_G \frac{dn_G}{dp_G}\,\delta\left(x_G - \frac{p_G}{p_2}\right) \quad (27)$$

$$= p_2 \sum_q \int_{x_{min}}^1 dx_2\, f_q(x_2) \left.\frac{dn_G}{dp_G}\right|_{p_G=x_Gp_2}, \quad (28)$$

where

$$x_{min} = \max\left[0, \frac{\lambda^2-m_q^2/p_2^2}{2\lambda}\right], \quad \lambda = x_G + \sqrt{x_G^2+\Lambda^2/p_2^2}. \quad (29)$$

These expressions give the distributions for prompt gluons in the interval $0 \le x_G \le x_{G\,max}$

$$x_{G\,max} = \frac{\mu^2-\Lambda^2/p_2^2}{2\mu}, \quad \mu = 1+\sqrt{1+m_q^2/p_2^2}. \quad (30)$$

Finally, we combine the expression (19) for the cross section for the elementary process with the distribution function $f_q(x_1)$ for the quark and the distribution dn_G/dx_G of the gluon to the cross section for the prompt ("P") process on the nucleon

$$\frac{d^2\sigma^P}{dMdy} = \frac{d^2\sigma_+^P}{dMdy} + \frac{d^2\sigma_-^P}{dMdy}, \quad (31)$$

where

$$\frac{d^2\sigma_+^P}{dMdy} = \sum_q \int_0^1 dx_1 f_q(x_1) \cdot\int_0^{x_{G\,max}} dx_G \frac{dn_G}{dx_G}\frac{d^2\sigma(qG\to l^+l^-X)}{dMdy}, \quad (32)$$

$$\frac{d^2\sigma_-^P}{dMdy} = \frac{d^2\sigma_+^P}{dMdy}(y \Rightarrow -y). \quad (33)$$

For nucleus-nucleus collisions the geometric factor has to take into account that points of gluon creation and interaction are different

$$\frac{d^2\sigma_{AB}^P}{dMdy} = \int d\mathbf{b}\int d\mathbf{s}\int_{-\infty}^{\infty} dz_A\,\rho_A(\mathbf{s},z_A)\int_{-\infty}^{\infty} dz_B\,\rho_B(\mathbf{b}-\mathbf{s},z_B) \times\sigma_{NN}^{in}\left[\int_{-\infty}^{z_A} dz\rho_A(\mathbf{s},z)\frac{d^2\sigma_-^P}{dMdy} + \int_{z_B}^{\infty} dz\rho_B(\mathbf{b}-\mathbf{s},z)\frac{d^2\sigma_+^P}{dMdy}\right]. \quad (34)$$

Again, expression (34) has to be divided by the total inelastic cross section to compare with experiment. Our results for proton (p-Be, p-Au) and heavy ion (Pb-Au) scattering are shown in Figs. 2, 3.

4 Conclusion

We have calculated two contributions to the spectrum of invariant masses of dileptons produced in proton-nucleus and nucleus-nucleus collisions. The direct production of dileptons $NN \to l^+l^-X$ and the production by $GN \to l^+l^-X$ from gluons which have been produced in another NN collision. Both processes happen during the early phase of hadronization and may be treated by pQCD on the partonic level - in contrast to the final stage of the

nuclear collision where hadrons and their decay into l^+l^- dominate.

The results of our calculations are summarized in Figs. 2 and 3: the mechanisms considered contribute to the observed spectrum less than 10% and therefore are unimportant on the present level of discussion. On this level also the theoretical uncertainties, for instance in the choice of the value for constituent quark mass or in the evaluation via two mechanisms (light cone *vs.* parton model) are not yet of importance.

We thank A.V. Tarasov for illuminating discussions. The work has been supported by the GSI under contract HD HÜF T and by the federal ministry BMBW under contract 06 HD 742.

References

1. G. Agakichiev et al. (CERES/NA45 and TAPS collaborations), Eur.Phys.J. **C4** (1998) 231
2. G. Agakichiev et al., CERES collaboration, Phys.Rev.Lett. **75** (1995) 1272; P. Wurm for the CERES collaboration, Nucl.Phys. **A590** (1995) 103c
3. N. Masera for the HELIOS-3 collaboration, Nucl.Phys. **A590** (1995) 93c
4. G.E. Brown and M. Rho, Phys.Rev.Lett. **66** (1995)
5. W. Cassing, W. Ehehalt and C.M. Ko, Phys.Lett. **B363** (1995) 35
6. G.Q. Li, C.M. Ko and G.E. Brown, Phys.Rev.Lett. **75** (1995) 4007; G.Q. Li, C.M. Ko, H. Sorge and G.E. Brown, Nucl.Phys. **A611** (1996) 539
7. J.V. Steele, H. Yamagishi and I. Zahed, Phys.Lett. **B384** (1996) 255; Phys.Rev. **D56** (1997) 5605
8. C. Song and V. Koch, Phys.Rev. **C54** (1996) 3218
9. R. Rapp, G. Chanfray and J. Wambach, Nucl.Phys. **A617** (1997) 472; G. Chanfray, R. Rapp and J. Wambach, Phys.Rev.Lett. **76** (1996) 368
10. B. Friman and H.J. Pirner, Nucl.Phys. **A617** (1997) 496
11. F. Klingl, N. Kaiser and W.Weise, Nucl.Phys. **A624** (1997) 527
12. W. Peters, M. Post, H. Lenske, S. Leupold and W. Mosel, Nucl.Phys. **A632** (1998) 109
13. J. Hüfner, B.Z. Kopeliovich, Phys.Lett. **B445** (1998) 223
14. R.D. Field, "Applications of Perturbative QCD", Addison-Wesley, 1989
15. B.Z. Kopeliovich, Proc. of the Workshop Hirschegg '95: *Dynamical Properties of Hadrons in Nuclear Matter*, Hirschegg January 16-21, 1995, ed. by H. Feldmeyer and W. Nörenberg, Darmstadt, 1995, p. 102 (hep-ph/9609385)
16. B.Z. Kopeliovich, A. Schäfer and A.V. Tarasov, Phys.Rev. **C59** (1999) 1609, extended version in hep-ph/9808378
17. B.Z. Kopeliovich, A. Schäfer, A.B. Tarasov, *Nonperturbative Effects in Gluon Radiation and Photoproduction of Quark Pairs*, hep-ph/9908245
18. H. De Vries, C.W. De Jager and C. De Vries, *Atomic Data and Nucl. Data Tables*, **36** (1987) 469
19. S.J. Brodsky, A. Hebecker and E. Quack, Phys.Rev. **D55** (1997) 2584
20. K. Golec-Biernat and M. Wüsthoff, Phys.Rev. **D58** (1998) 074010; K. Golec-Biernat and M. Wüsthoff, hep-ph/9903358
21. B.Z. Kopeliovich and B.G. Zakharov, Phys.Rev. **D44** (1991) 3466